

Measurements of D^0 production and of decay branching fractions in neutrino nucleon scattering

CHORUS Collaboration

Abstract

During the years 1994–97, the emulsion target of the CHORUS detector was exposed to the wide-band neutrino beam of the CERN SPS of 27 GeV average neutrino energy. In total about 100 000 charged-current neutrino interactions were located in the nuclear emulsion target and fully reconstructed. From this sample of events which was based on the data acquired by new automatic scanning systems, 1048 charged-current interactions with a D^0 in the final state were selected by a pattern recognition program and confirmed as neutral-particle decays through visual inspection. The ratio of decay branching fractions of the D^0 into four charged particles to two charged particles was measured to be $B(D^0 \rightarrow V4)/B(D^0 \rightarrow V2) = 0.207 \pm 0.016 \pm 0.004$. The inclusive measurement of the observed production rate of the D^0 with a decay into four charged prongs in combination with external measurements of this topological branching ratio was used to determine the total D^0 production rate by neutrinos without additional assumption on the branching fractions. The value of this rate relative to the charged-current cross-section was found to be $\sigma(D^0)/\sigma(CC) = 0.0269 \pm 0.0018 \pm 0.0013$. In addition, the same normalization method was used to deduce the inclusive topological decay rate into final states with neutral particles only. A value of $0.218 \pm 0.049 \pm 0.036$ was found for this branching fraction. From an observed number of three charged six-prong events the branching ratio into six charged particles was determined to be $(1.2_{-0.9}^{+1.3} \pm 0.2) \times 10^{-3}$. A measurement of the energy dependence of the D^0 production by neutrinos relative to the total charged-current cross-section is also reported. This measurement was used to deduce for m_c , the effective charm-quark mass, a value of $(1.42 \pm 0.08) \text{ GeV}/c^2$.

To be published in Physics Letters B

CHORUS Collaboration

G. Önengüt

Çukurova University, Adana, Turkey

R. van Dantzig, M. de Jong, R.G.C. Oldeman¹

NIKHEF, Amsterdam, The Netherlands

M. Güler, U. Köse, P. Tolun

METU, Ankara, Turkey

M.G. Catanesi, M.T. Muciaccia

Università di Bari and INFN, Bari, Italy

K. Winter

Humboldt Universität, Berlin, Germany²

B. Van de Vyver^{3,4}, P. Vilain⁵, G. Wilquet⁵

Inter-University Institute for High Energies (ULB-VUB) Brussels, Belgium

B. Saitta

Università di Cagliari and INFN, Cagliari, Italy

E. Di Capua

Università di Ferrara and INFN, Ferrara, Italy

S. Ogawa, H. Shibuya

Toho University, Funabashi, Japan

I.R. Hristova⁶, A. Kayis-Topaksu⁷, T. Kawamura, D. Kolev⁸, H. Meinhard, J. Panman, A. Rozanov⁹,

R. Tsenov⁸, J.W.E. Uiterwijk, P. Zucchelli^{3,10}

CERN, Geneva, Switzerland

J. Goldberg

Technion, Haifa, Israel

M. Chikawa

Kinki University, Higashiosaka, Japan

J.S. Song, C.S. Yoon

Gyeongsang National University, Jinju, Korea

K. Kodama, N. Ushida

Aichi University of Education, Kariya, Japan

S. Aoki, T. Hara

Kobe University, Kobe, Japan

T. Delbar, D. Favart, G. Grégoire, S. Kalinin, I. Makhlioueva

Université Catholique de Louvain, Louvain-la-Neuve, Belgium

A. Artamonov, P. Gorbunov, V. Khovansky, V. Shamanov, I. Tsukerman

Institute for Theoretical and Experimental Physics, Moscow, Russian Federation

N. Bruski, D. Frekers

Westfälische Wilhelms-Universität, Münster, Germany²

K. Hoshino, J. Kawada, M. Komatsu, M. Miyanishi, M. Nakamura, T. Nakano, K. Narita, K. Niu,

K. Niwa, N. Nonaka, O. Sato, T. Toshito

Nagoya University, Nagoya, Japan

S. Buontempo, A.G. Cocco, N. D'Ambrosio, G. De Lellis, G. De Rosa, F. Di Capua, G. Fiorillo,

A. Marotta, M. Messina, P. Migliozi, L. Scotto Lavina, M. Sorrentino, P. Strolin, V. Tioukov

Università Federico II and INFN, Naples, Italy

T. Okusawa

Osaka City University, Osaka, Japan

U. Dore, P.F. Loverre, L. Ludovici, G. Rosa, R. Santacesaria, A. Satta, F.R. Spada

Università La Sapienza and INFN, Rome, Italy

E. Barbuto, C. Bozza, G. Grella, G. Romano, C. Sirignano, S. Sorrentino

Università di Salerno and INFN, Salerno, Italy

Y. Sato, I. Tezuka

Utsunomiya University, Utsunomiya, Japan

¹ Now at University of Liverpool, Liverpool, UK

² Supported by the German Bundesministerium für Bildung und Forschung under contract numbers 05 6BU11P and 05 7MS12P.

³ Now at SpinX Technologies, Geneva, Switzerland.

⁴ Fonds voor Wetenschappelijk Onderzoek, Belgium.

⁵ Fonds National de la Recherche Scientifique, Belgium.

⁶ Now at DESY, Hamburg.

⁷ On leave of absence from Çukurova University, Adana, Turkey.

⁸ On leave of absence and at St. Kliment Ohridski University of Sofia, Bulgaria.

⁹ Now at CPPM CNRS-IN2P3, Marseille, France.

¹⁰ On leave of absence from INFN, Ferrara, Italy.

1 Introduction

Charm production in ν_μ and $\bar{\nu}_\mu$ charged-current interactions has been studied over the years in several experiments [1-7], mainly through the analysis of the so-called dimuon events. In these, the non-leading muon is assumed to be the product of the decay of a short-lived particle, charged or neutral, meson or baryon, containing a charmed quark. Experiments of this type, however, are affected by a large background from the decay in flight of pions and kaons. In addition they have to rely upon the knowledge of the relative content of the different charmed particles' species in the final state as well as of their decay branching fractions into states containing a muon.

On the other hand, poor statistics has been in the past the limiting factor of neutrino experiments where specific charmed particles are identified. This problem has been partially overcome in CHORUS, however, and recently it has become possible to study production of individual charm species with hundreds of events [8].

While neutrino experiments have contributed to establish the production of charmed particles, in particular of charmed baryons [9-16], the determination of lifetimes and relative branching fractions remains without doubt the domain of e^+e^- and photo- and hadro-production experiments. This is indeed the case for the D^0 , whose lifetime and some of its branching fractions (both in Cabibbo favoured and suppressed channels) have been measured to an extremely high degree of accuracy. Recent high-precision measurements were reported by the photo-production experiment FOCUS [17].

Yet, the sum of the measured decay widths is only 64% of the total [18]. This is explained by observing that some exclusive decay modes – mostly involving more than one neutral particle – remain unmeasured, since the D^0 identification relies very often on the reconstruction of the invariant mass, thus forcing a 'guessing' of the partial width into these channels [19].

In a previous paper [8] we presented a measurement of the ratio $\sigma(D^0)/\sigma(CC)$ with decays of the D^0 into two or four charged particles. In this paper, with an increased statistics corresponding to the complete event sample, we measure the *total* D^0 production rate in νN charged-current interactions and, using the energy dependence of this rate, obtain a value for m_c , the effective mass of the charm quark. In addition, we measure the branching fraction of D^0 into six charged particles. Even though the statistics can not compete with that of e^+e^- and photo- and hadro-production experiments, taking advantage of the *inclusive* character of the measurement, we estimate the decay branching fraction of D^0 into final states with neutral particles only.

The method used for the analysis is based on the observation that the topological branching fraction of the D^0 into four charged prongs can be obtained by the sum of all known individual channels, and that measurements for all relevant decay channels are available in the literature [18]. The missing decay modes are those with two neutral particles in the final state. Their contribution can be estimated to be of the same order as the charged six-prong modes and is therefore negligible. The situation for the two-prong decay modes is quite different. The contribution of unknown modes is estimated to be significant [19] and is of the order of the branching ratio into four charged particles. Therefore to use the topological branching fraction into four prongs is the most reliable method for obtaining an absolute normalization. This allows us to deduce the branching ratio into fully neutral final states from our inclusive measurement of the ratios of observed charged two-prong ('V2'), four-prong ('V4'), and six-prong ('V6') events. In addition, the same observation makes it possible to determine a production cross-section for the D^0 without further assumption concerning its decay branching ratios.

2 The experimental set-up

The CHORUS detector was exposed to the wide-band neutrino beam of the CERN SPS during the years 1994–97. The beam consisted mainly of ν_μ with a contamination of 5% $\bar{\nu}_\mu$ and about 1% ν_e . In total $\approx 94\,000$ ν_μ CC events with a negative primary muon were located and fully reconstructed in the emulsion target.

The CHORUS detector is a hybrid set-up which combines a nuclear emulsion target with various electronic detectors such as trigger hodoscopes, a scintillating fibre tracker system, a hadron spectrometer, electromagnetic and hadronic calorimeters, and a muon spectrometer [20]. The hadron spectrometer measures the bending of charged particles using an air-core magnet, the calorimeter is used to determine the energy of showers, and the muon spectrometer determines the charge and momentum of muons.

Tracks reconstructed in the scintillating fibre detectors are followed upstream in the beam direction to locate the interaction vertices in the emulsion target. The nuclear emulsion is used as a target for neutrino interactions, and to visualize a precise three-dimensional reconstruction of the vertex region of the events.

The emulsion target has an overall mass of 770 kg and is segmented into four stacks. Each stack consists of eight modules of 36 plates of size of 36 cm \times 72 cm. Each plate has a 90 μ m plastic base coated on both sides with a 350 μ m emulsion layer. Each stack is followed by three interface emulsion sheets having a 90 μ m emulsion layer on both sides of a 800 μ m thick plastic base and by a set of scintillating fibre target-tracker planes. The interface emulsion sheets and the fibre tracker system provide accurate particle trajectory predictions with a precision of about 150 μ m in position and 2 mrad in the track angle.

The emulsion scanning is performed by computer-controlled, fully automatic microscope stages equipped with a CCD camera and a read-out system called ‘track selector’ [21, 22]. In order to recognize track segments in the emulsion, a series of tomographic images are taken by focusing at different depths in the emulsion layer. The digitized images are shifted according to the predicted track angle and then added. The presence of aligned grains forming a track is detected as a local peak of the grey-level of the summed image. In the absence of an angular prediction, all angles smaller than 400 mrad are tried by parallel processing hardware. The track-finding efficiency of the track selector is higher than 98% for track slopes less than 400 mrad [23].

3 Event reconstruction

The event reconstruction starts with the pattern recognition in the electronic detectors. Tracks are found in the fibre-trackers in the target region and, independently, in the muon spectrometer. A matching is attempted between these two sets of tracks in order to identify primary muons. Vertices are defined using the points of closest approach of the fibre-tracker tracks (‘TT-tracks’). The primary vertex is the most upstream one that contains a muon. Such a muon is defined as primary muon, and used as the so-called ‘scan-back’ track. The impact point of the scan-back track is predicted on the most downstream interface emulsion sheets. The emulsion data-taking starts with the search for all scan-back tracks collected for the entire exposure within an area of 1 mm² centred around each TT-track prediction. Emulsion tracks are selected as candidates to be followed further upstream on the basis of the precise alignment of the interface sheets with respect to the fibre-trackers. This alignment is obtained by finding the best match of the full set of predicted tracks with the full set of found candidates. The most selective parameter is the direction of the predicted track. Once found, the set of scan-back tracks are followed upstream from one plate to the next within a strongly reduced scanning area as the resolution improves. Within the emulsion stacks, the scanning area reduces to a square with 50 μ m sides. As the scanning procedure continues, the plate-to-plate alignment is obtained by a coarse adjustment with reference marks refined by track maps measured in adjacent plates. The ‘vertex plate’ is defined as the first (most downstream) of two consecutive plates where the scan-back track is not detected. This ‘event location’ process is described in detail in Refs. [23] and [24].

Once the vertex plate is identified, a very fast scanning system [25] is used to perform a detailed analysis of the emulsion volume around the vertex position, recording, for each event, all track segments within a given angular acceptance. We refer to this type of scanning, originally developed for the DONUT experiment [26], as ‘NetScan’ data taking [27]. The procedure is described in detail in Ref. [23].

In the CHORUS experiment, the scanning volume is 1.5 mm wide in each transverse direction and 6.3 mm along the beam direction, corresponding to eight emulsion plates. This volume contains the vertex plate itself, the plate immediately upstream, and the six plates downstream from the vertex plate. The plate upstream of the vertex acts as a veto for passing through tracks. The six plates downstream of the vertex act as decay space and are used to detect the tracks of the decay daughters. The scanning area is centred on the extrapolated transverse position of the scan-back track. The angular acceptance corresponds to a cone of 400 mrad half-aperture aligned along the beam direction.

The first step of the NetScan event reconstruction is the selection of only those segments belonging to the neutrino interaction under study out of the large number of track segments reconstructed. A coarse plate-to-plate alignment is performed by comparing the pattern of segments in a plate with the corresponding pattern in the next upstream plate. With this coarse alignment each segment found on one

Table 1: Charged-current data sample and charm subsample

Located CC events	93 807
Selected for visual inspection	2752
Decay topologies with flight length $< 25 \mu\text{m}$	3
Topologies with kink angle $< 50 \text{ mrad}$	11
Secondary interactions	278
Electron–positron pairs	95
Overlay neutrino interactions	44
Uncorrelated (overlay) secondary vertices	21
Passing-through tracks	128
All tracks from primary vertex	142
δ -rays	2
Other	15
Charged charm candidates	965
V2	819
V4	226
V6	3
Total charm candidates	2013

plate is extrapolated to the next plate where a matching segment is looked for within about $4 \mu\text{m}$ (3σ of alignment resolution) in position and 20 mrad in angle. If none is found the straight-line extrapolation is tried one plate further upstream.

A second and more accurate inter-plate alignment is performed using tracks passing through the entire volume after the connection of all matched segments. These tracks are mainly coming from muons associated with the neutrino beam or charged-particle beams in the same experimental area. After this fine alignment, the distribution of the residual of the segment positions with respect to the fitted track has an r.m.s. width of about $0.45 \mu\text{m}$. At this stage, typically about 400 tracks remain in the volume. The majority of these are tracks of low-momentum particles (mainly Compton electrons and δ -rays) with momentum less than $100 \text{ MeV}/c$. These background tracks are rejected with a criterion based on the χ^2 of a straight-line fit to the track segments. The final step is the rejection of all tracks not originating from the scanning volume. After this filtering, the mean number of tracks originating in the scan volume is about 40.

The reconstruction algorithm then tries to associate the remaining tracks to common vertices. A track is attached to a vertex if the distance of the vertex point to the reconstructed track (called hereafter impact parameter) is less than $10 \mu\text{m}$. At the end of the procedure, one defines a primary vertex (and its associated tracks) and possibly one or more secondary vertices to which ‘daughter tracks’ are attached.

Once the event is reconstructed, the charged-current candidates are further analysed and secondary vertices are recognized. An event is defined as a candidate for a charged-current neutrino interaction if the primary muon track, defined by the electronic detectors, is found in more than one emulsion plate. Decay topologies are selected with the following criteria. At least one of the tracks connected to a secondary vertex is detected in more than one plate, and the direction measured in the emulsion matches that of a track reconstructed in the fibre tracker system. The parent angle, in the case of a neutral particle decay deduced from the line connecting the primary and secondary vertex, should be within 400 mrad from the beam direction. The impact parameter to the primary vertex of at least one of the daughter tracks is larger than a value which is determined on the basis of the resolution, which depends on the track angle with respect to the beam, θ^1 . In order to remove random association, the impact parameter is also required to be smaller than a value depending on the distance over which the track is extrapolated to the vertex. The typical tolerance is $130 \mu\text{m}$. The flight length of the parent candidate should be more than $25 \mu\text{m}$.

From the current sample of 93 807 scanned and analysed neutrino-induced charged-current events,

¹⁾ The resolution to extrapolate to the vertex is $\sigma = \sqrt{0.003^2 + (0.0194 \cdot \tan \theta)^2}$.

these criteria select 2752 events as having a decay topology. These have been visually inspected (‘eye-scan’) to confirm the presence of a decay. A secondary vertex is accepted as a decay if the number of charged particles is consistent with charge conservation and no other activity (Auger-electron or visible recoil) is observed. Only those events are used in which the secondary vertex is consistent with the decay of a neutral particle. Thus the selection and identification of the D^0 sample used in this analysis is based on the decay topology of the D^0 alone.

The result of the visual inspection is given in Table 1. The purity of the automatic selection is 73.2%. The rejected sample consists of secondary hadronic interactions, δ -rays or gamma conversions, overlay neutrino interactions, and of low-momentum tracks which, due to multiple scattering, appear as tracks with a large impact parameter. The remainder consists either of false vertices, being reconstructed using one or more background tracks, or of vertices with a parent track not connected to the primary (passing-through tracks).

4 Reconstruction efficiency and background evaluation

The efficiency of the event reconstruction in the electronic detector and the event location and reconstruction in the emulsion needs to be evaluated in order to determine cross-sections of the processes under study. The steps which have to be simulated are:

- the properties of the neutrino beam and the neutrino interaction in the target,
- the pattern recognition in the electronic tracking detectors,
- the definition of the scan-back track,
- the event location technique in the emulsion,
- the pattern recognition in the emulsion and
- the selection of candidates.

The event location procedure is sensitive to random losses in the scanning procedure due to imperfections in the emulsion plates, which lead to a loss of efficiency. Two situations can occur: during the plate-to-plate scan-back procedure a background track has been followed, or the scan-back track has been missed on more than one consecutive plate. In the first case this leads to the choice of a through-going track and no vertex is located. In the latter case an incorrect vertex plate is found where no interaction vertex can be reconstructed. The size of this random loss is difficult to simulate with precision. However, in both cases, this loss of location efficiency is unbiased with respect to the details of the event being looked for, except for a dependence on the momentum and angle of the scan-back track. In charged-current interactions the muon is always chosen for that purpose. The strategy of the measurements is therefore to determine *ratios* of rates, either between different D^0 decay topologies or between D^0 and CC rates. This strategy also has the advantage that, for the other efficiency components, only ratios need to be determined, thereby significantly reducing the systematic error.

Ratios of the efficiencies in reconstructing and selecting neutral charmed hadrons and charged-current interactions used for the normalization have therefore to be determined. The neutrino beam spectrum is simulated using the GBEAM [28] generator based on GEANT3 [29]. The calculation of the prediction of ν_μ in the beam is improved by using measurements of hadron production performed by the SPY/NA56 experiment [30] and by adjusting the simulation to reproduce all components where the signal is not expected. This procedure was developed within the NOMAD experiment [31]. When the neutrino scatters off a nucleon, different physical mechanisms produce charmed hadrons, however, D^0 's are predominantly produced in deep-inelastic interactions. Several Monte Carlo generators are used [32]. Inclusive CC interactions relevant for the normalization have to be described by simulating quasi-elastic and deep-inelastic processes. Deep-inelastic scattering interactions are simulated using the JETTA generator [33] which is based on LEPTO 6.1 [34] and JETSET [35]. This generator is used to simulate charm-production as well as inclusive CC interactions used for the normalization. Quasi-elastic interactions and resonance production processes are simulated with the RESQUE generator [36]. The simulation of the detector response for each process is performed by a GEANT 3 based simulation program.

The simulated response of the electronic detectors is processed through the same analysis chain as the raw data obtained with the detector. The simulation of the emulsion response can be divided into two parts: event location and event selection. The event location efficiency describes the shortcomings of

Table 2: Selection efficiencies and overall efficiencies relative to CC for different decay topologies

Decay topology	Selection efficiency after reconstruction	Overall efficiency relative to CC
$D^0 \rightarrow V2$	0.561 ± 0.018	0.483 ± 0.012
$D^0 \rightarrow V4$	0.754 ± 0.027	0.650 ± 0.019
$D^0 \rightarrow V6$	0.80 ± 0.18	0.69 ± 0.16
All D^0 decay modes		0.401 ± 0.027

finding charged-current interactions in emulsion. This efficiency is approximated by a parametrization which is a function of the primary muon momentum and slope.

In order to evaluate the NetScan efficiency, realistic conditions of track densities in the emulsion have to be reproduced. These are obtained by merging the emulsion data of the simulated events with real NetScan data which do not have a reconstructed vertex but contain tracks which stop or pass through the NetScan fiducial volume. These so-called ‘empty volumes’ represent a realistic background. The combined data are passed through the same NetScan reconstruction and selection programs as used for real data. The need to use measured empty volumes imposes a limitation to the statistics which can be produced with the simulation. The details of the response of the automatic microscopes are used as input into this calculation. Important parameters are the angular resolution and efficiency as function of incident angle of the track. The spread in the performance of the microscopes is found to induce a difference of $\pm 2\%$ in the calculation of the selection efficiencies for the charm detection. This variation is correlated for the different decay topologies, so that ratios of efficiencies are less affected. However, in the comparison between the detection of CC events and the more subtle selection of the decay signatures the detailed resolution of the microscopes plays a role. The weighted average performance of the individual microscope stages is taken for the calculation in order to minimize the uncertainty. Taking into account this instrumental effect and other factors, such as the uncertainty in the fragmentation, we estimate a total systematic uncertainty in the efficiency of 2% when different D^0 decay topologies are compared and 4% when inclusive CC event detection is compared with charm detection. It was observed that the strongest dependence on the efficiency is given by the energy spectrum of the produced D^0 's. In an earlier publication the energy spectrum of the D^0 's in the same event sample was compared with the simulation and found to be compatible [37]. The selection efficiencies for different decay topologies (after reconstruction) and the relative overall efficiencies compared to CC interactions are shown in Table 2. The value quoted for the overall efficiency in detecting D^0 's takes into account the branching ratios measured in this analysis, including unmeasured decay topologies, and the corresponding additional uncertainties.

The energy dependence of the efficiency for the D^0 reconstruction is shown in Figure 1. As a result of the requirement that at least one track of the secondary vertex be matched with a track in the electronic detectors, the efficiency for four-prongs is higher than for two-prongs. Since the simulation contains too few six-prong events to determine their energy dependence, this dependence is assumed to be equal to the one for four-prongs scaled with the average efficiency for six-prongs. This approximation has a negligible effect on the final result owing to the small value of this branching ratio. The overall reconstruction efficiency for the D^0 is lower than the individual two- and four-prong efficiency because of the admixture of the decays into a fully neutral final state which are not detected in this experiment.

Possible background sources for D^0 decays are mainly electron–positron pairs and decays of strange particles. An electron–positron pair can be tagged as a D^0 decay if the opening angle is large. Since the momentum of these electrons is very low in this case, at least one of them is scattered within a few plates downstream of the decay vertex. So, this background is eliminated by following the decay daughter which does not match a TT track. Neutral strange particle decays such as Λ^0 and K_s^0 induce a background which is small owing to their much longer decay length. Their effect is determined by simulating neutral strange particle production in deep-inelastic processes using the JETTA generator. The simulated production rate is consistent with measurements from the NOMAD experiment in the same neutrino beam [38] within 9% and 16% for K_s^0 and Λ^0 production, respectively. Part of this difference is

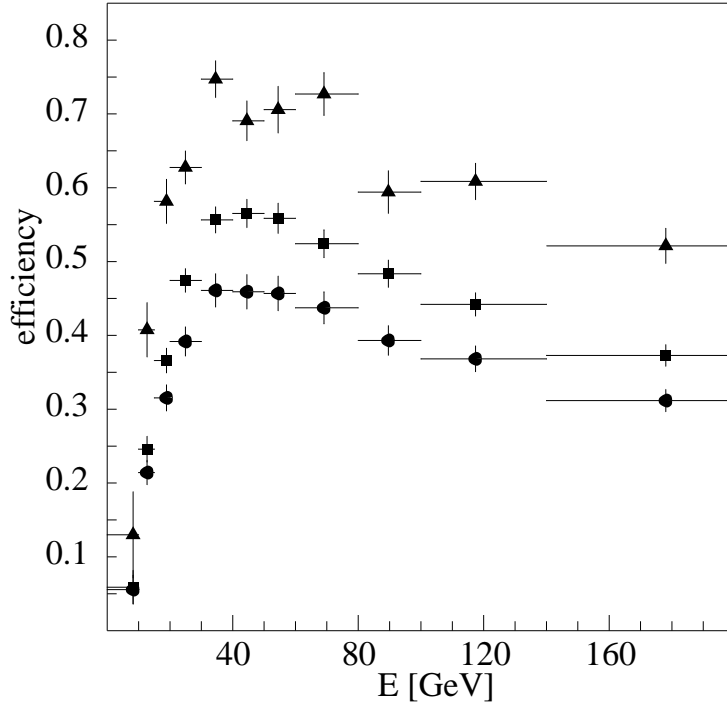


Figure 1: Ratios of the efficiency for the detection of D^0 's relative to CC interactions as function of neutrino energy. The data points indicated with circles show the overall efficiency for D^0 detection, the points marked with triangles and squares the efficiency for four-prongs and two-prongs, respectively.

explained by the slightly lower average energy in the NOMAD measurements. The full simulation of the electronic detectors and of the event reconstruction in the emulsion is used to calculate the background from these neutral strange particle decays [39]. The number of events is evaluated to be $11.5 \pm 1.9 \Lambda^0$'s and $25.1 \pm 2.9 K_S^0$'s, respectively. This background is only present in the D^0 decays into two prongs.

Other sources of backgrounds are interactions of neutral particles without visible activity. A secondary vertex is recognized as an interaction of a neutral particle by visible activity at the interaction point or by failing the requirement of charge conservation for decays. Their number was estimated from an analysis of 21 identified neutral interactions within the same data sample. This sample contains events with one up to five prongs at the secondary vertex. From the 12 interactions with an odd number of prongs, only one event shows no activity. From these numbers we estimate that the background from this source in the two-prong D^0 sample is 0.5 ± 0.5 events, and in the four-prong D^0 sample is 0.25 ± 0.25 events. For the six-prong sample, only an upper limit of 0.19 events can be derived at 90% C.L.

The Dalitz decay of the π^0 causes a small migration of n -prongs into the topological class with $n + 2$ charged particles. Using the value of $(1.198 \pm 0.032)\%$ [18] for this decay rate, this effect is calculable with sufficient precision.

The migration of the neutral decay modes into the class of two charged prongs is small – less than one event – because the efficiency to match an electron or positron to a TT track is reduced due to the showering of these particles. Using the average number of π^0 's in the two-prong decay modes, a contribution of 7.3 ± 1.5 two-prong events to the four prongs is calculated. The efficiency in detecting these decays is similar to two-prong decays. With an accumulated branching fraction of 4.3% for the four charged prongs with an additional π^0 (see Table 3), one predicts that 0.84 ± 0.1 event migrates into the six-prong class. This constitutes the largest background to this sample. The systematic errors in these numbers are the combination with roughly equal weight of the statistics of the number of observed decays, the knowledge of the decay fractions into modes with extra π^0 's in D^0 decays and the detection efficiency.

Table 3: The decay modes used in the calculation of $B(D^0 \rightarrow V4)$

D⁰ decay mode	Branching fraction
$K^- \pi^+ \pi^+ \pi^-$	0.0746 ± 0.0031
$K^- \pi^+ \pi^+ \pi^- \pi^0$	0.040 ± 0.004
$\overline{K}^0 \pi^+ \pi^+ \pi^- \pi^-$	0.0064 ± 0.0018
$\pi^+ \pi^+ \pi^- \pi^-$	0.0073 ± 0.0005
$K^+ K^- \pi^+ \pi^-$	0.00249 ± 0.00023
$K^+ K^- \pi^+ \pi^- \pi^0$	0.0031 ± 0.002
All four prongs	0.1339 ± 0.0061

5 D⁰ decay branching fractions and production rate

The ratios of topological D⁰ branching fractions can be obtained by correcting the observed numbers of events with their corresponding efficiencies and background. For the ratio of four prongs, $B(D^0 \rightarrow V4)$, to two prongs, $B(D^0 \rightarrow V2)$, we find:

$$B(D^0 \rightarrow V4)/B(D^0 \rightarrow V2) = 0.207 \pm 0.016 \pm 0.004, \quad (1)$$

using the efficiency ratio $\varepsilon(D^0 \rightarrow V4)/\varepsilon(D^0 \rightarrow V2) = 1.34 \pm 0.03 \pm 0.03$.

In a notation that will be used throughout, the first error is statistical and the second systematic. The main component of the statistical error is given by the event statistics however, the limited statistics of the simulation is also taken into account in this error component, a convention which has been used for all results. The systematic error is an estimate of the uncertainty in the ratio of the detection efficiency for four prongs and two prongs ($\pm 2\%$). The background mentioned in Section 4 has been subtracted from the sample of two-prong candidates. Owing to their small number, the systematic error is negligible compared to the uncertainty in the efficiency ratio. The value is in good agreement with our previous measurement, 0.23 ± 0.04 , obtained on a partial sample reported in Ref. [8].

Even though the sum of the D⁰ branching fractions has a large unmeasured part, the total of the measured exclusive channels being about 64% [18, 19], the fraction of decays into four charged particles is measured with a 4.6% relative accuracy and found to be $B(D^0 \rightarrow V4) = 0.1339 \pm 0.0061$ [18]. The considered decay modes are shown in Table 3. The correlation between the measurements of the first two modes has been taken into account. Missing decay modes are those with four charged and two neutral daughter particles. Their contribution can be estimated from the total rate of six charged prongs, which is negligible when compared with the error.

The precision of this external measurement, together with the observed number of D⁰ decays into four charged hadrons, can be exploited to yield the ratio of the cross-sections $\sigma(D^0)/\sigma(CC)$, where the decays of D⁰ include also modes which are not detectable in CHORUS. The external information provided by the value of $B(D^0 \rightarrow V4)$ also allows the measurements of absolute branching fractions to be made using ratios with respect to this decay topology.

The topological branching fraction into two charged particles can be obtained using the external measurement of $B(D^0 \rightarrow V4)$ and the ratio reported in Eq. (1). We find a value

$$B(D^0 \rightarrow V2) = 0.647 \pm 0.049 \pm 0.031. \quad (2)$$

The systematic error is dominated by the uncertainty in the value of $B(D^0 \rightarrow V4)$. Summing all measured decay modes with two charged daughters in the literature, one finds a value $B(D^0 \rightarrow V2) = 0.485 \pm 0.020$ [18]. The difference does not represent a discrepancy, since in this experiment the inclusive two-prong decay mode is measured; while the latter branching fraction is the sum of all exclusive channels for which measurements exist. However, as pointed out by Wohl [19], the importance of the unmeasured modes (mostly consisting of states with two or more neutral particles) can be ‘guessed’ by comparing similar channels involving charged particles. For instance $D^0 \rightarrow K^- \pi^+ \pi^0 \pi^0$ and $D^0 \rightarrow \overline{K}^0 \pi^0 \pi^0 \pi^0$ are not measured. Their branching fractions can be ‘guessed’ to be equal to the

measured sum of the $D^0 \rightarrow K^- \pi^+ \pi^+ \pi^-$ and $D^0 \rightarrow \overline{K}^0 \pi^+ \pi^- \pi^0$ branching fractions. In this procedure isospin is used even though this is not strictly applicable to weak decays (hence the use of the word ‘guessing’.) With this method a value of $B(D^0 \rightarrow V2) = 0.636 \pm 0.026 \pm$ (guess uncertainty) is obtained, in agreement with the measurement quoted in Eq. (2). It should be noted that the uncertainty in the guessed modes has not been included in the first error, except for a scaling factor, and an additional inherent uncertainty in the extrapolation to unmeasured modes has been indicated generically by the error marked ‘guess uncertainty’. Similarly, for the ratio $B(D^0 \rightarrow V4)/B(D^0 \rightarrow V2)$ summing all measured modes, one finds a value 0.276 ± 0.017 , while correcting for unmeasured branching ratios a value $0.211 \pm 0.013 \pm$ (guess uncertainty) is obtained, again in good agreement with our direct determination given in Eq. (1).

Three events were observed with six charged daughter tracks. Using again the normalization of the total decay width provided by the external knowledge of $B(D^0 \rightarrow V4)$ and taking into account the background of four prongs with Dalitz decays of the π^0 and the estimate of the background coming from neutral strange particle decays, one obtains a value of the branching ratio into six prongs

$$B(D^0 \rightarrow V6) = (1.2_{-0.9}^{+1.3} \pm 0.2) \times 10^{-3} . \quad (3)$$

The statistical error is determined following the procedure described in Ref. [40] and has the meaning of a 68% confidence interval. The systematic error is given by the uncertainty in the background and in the efficiency determination. This measurement is in agreement with previous measurements of exclusive modes in hadro-production [41] and photo-production [42] experiments. The recent and more precise measurement reported by FOCUS [42] gives a value for the sum of all observed modes $B(D^0 \rightarrow V6) = (0.59 \pm 0.12) \times 10^{-3}$. Within the errors, our measurement is compatible with the latter number and also gives a limit to the strength of modes not observed in the exclusive measurements. The small value for the charged six-prong branching fraction given in Eq. (3) justifies our approximation to neglect the modes with two neutral daughters in the normalization based on four prongs.

From the results of the branching fractions into visible decays mentioned above, the branching ratio into final states with all neutral daughters can be deduced using the equation:

$$B(D^0 \rightarrow V0) = 1 - B(D^0 \rightarrow V4) \left[1 + \frac{B(D^0 \rightarrow V2)}{B(D^0 \rightarrow V4)} + \frac{B(D^0 \rightarrow V6)}{B(D^0 \rightarrow V4)} \right] . \quad (4)$$

We obtain the result:

$$B(D^0 \rightarrow V0) = 0.218 \pm 0.049 \pm 0.036 . \quad (5)$$

The main component of the statistical error is given by the propagation of the error in the number of four-prong events while the main contribution of the systematic error is the uncertainty in $B(D^0 \rightarrow V4)$. This result is significantly larger than the sum of measured neutral decay modes [18] ($\approx 5\%$). However, in this case as well, Wohl predicted a result of $\approx 25\%$ in agreement with this measurement [19].

As mentioned above, the relative production cross-section of D^0 's in CC interactions with respect to the inclusive CC cross-section can be obtained without making assumptions concerning the branching fractions of the D^0 by using the observed number of decays into four prongs and $B(D^0 \rightarrow V4)$. This approach minimizes the systematic uncertainty at the expense of the statistical error. The ratio of efficiencies for the detection of D^0 's decaying into four prongs and CC events was estimated to be $\varepsilon(D^0 \rightarrow V4)/\varepsilon(CC) = 0.650 \pm 0.013 \pm 0.015$. With the statistics given in Table 1 a value of:

$$\sigma(D^0)/\sigma(CC) = 0.0269 \pm 0.0018 \pm 0.0013 , \quad (6)$$

for the relative rate compared to CC is obtained. The statistical error is dominated by the limited V4 sample with a negligible contribution of the CC normalization. The systematic error is mainly given by two components: the uncertainty in the external knowledge of $B(D^0 \rightarrow V4)$ and the ratio of the efficiencies of four-prong D^0 events and CC interactions which is known to 3%.

The result quoted in Eq. (6) is consistent with our previous measurement $\sigma(D^0)/\sigma(CC) = 0.0199 \pm 0.0013 \pm 0.0017$ [8], which only considered the branching ratios into two and four prongs [8]. Using the

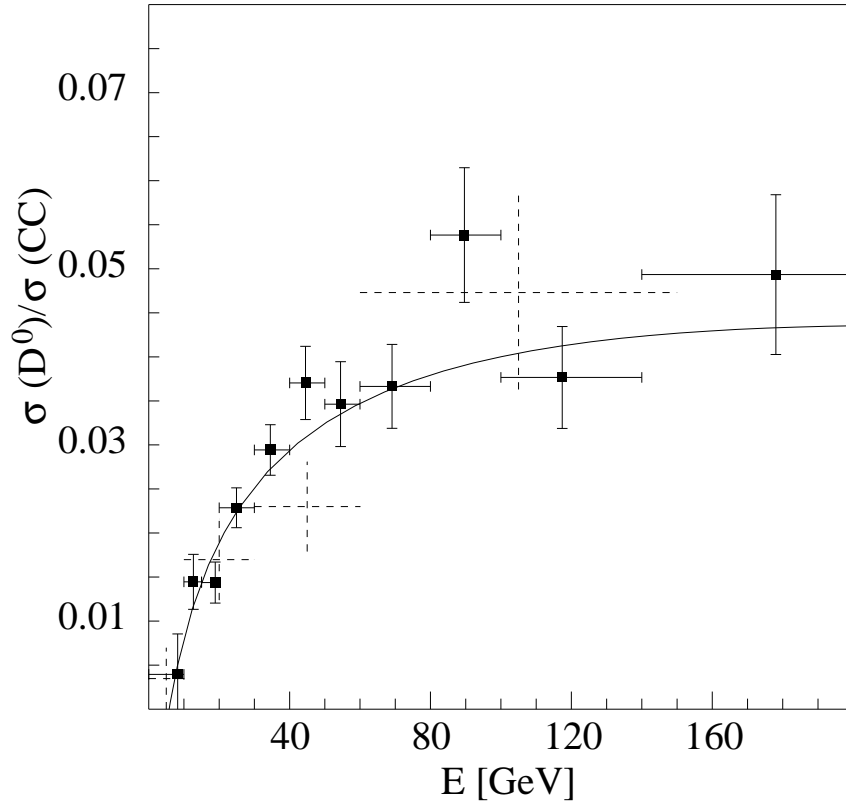


Figure 2: Energy dependence of the cross-section ratio. The data points drawn as full lines show the measurements reported here, the dashed lines the E531 [44] results. The curve through the data points shows the result of the model calculation as described in the text.

measurement of $B(D^0 \rightarrow V0)$ given in Eq. (5), the central value of the previous measurement can be translated to include all decay modes to the value 0.025.

The statistical error of the present measurement is given by the number of four-prong decays only, and is therefore larger than the statistical error of the previous measurement which was obtained using all decay-events. However, the procedure used in the present analysis allows the total production rate to be measured without assumption concerning the invisible decay modes.

The energy dependence of the D^0 production cross-section relative to the CC interaction rate was obtained by estimating the energy of the interacting neutrino on an event-by-event basis. A good estimate is the sum of the energy of the primary muon and the total energy deposition in the calorimeter corrected for the energy deposited by the muon and for the unmeasured energy loss of hadrons in the material upstream of the calorimeter. This unmeasured part is mainly due to the absorption in the emulsion stacks and is corrected as function of the measured vertex position. The resolution of the calorimeter energy measurement is $\sigma(E)/E = (0.323 \pm 0.024)/\sqrt{E/\text{GeV}} + (0.014 \pm 0.007)$ [20]. The momentum resolution varies from $\approx 15\%$ [43] in the 12–28 GeV/c interval to 19% [20] at about 70 GeV/c, as measured with test-beam muons. Events are summed in bins of estimated energy irrespective of their decay topology. Owing to the relatively small size of the energy bins, the average neutrino energy is very similar for charm production events and CC events within the same bin, and no correction is necessary. The efficiency is calculated by weighting the energy-dependent and decay topology-dependent efficiencies with the measured branching ratios as reported above. This procedure also corrects the total cross-section for the unmeasured neutral decay modes. The energy dependence of the detection efficiencies is given in Figure 1. The measurement of the D^0 production rate relative to the CC interaction rate is shown as function of neutrino energy and compared with the measurement from E531 [44] in Figure 2. The E531 points are drawn using their total charged and neutral charm particle production rate scaled to their overall cross-section for the D^0 , and are in good agreement with the present measurements.

Table 4: Fit parameters for the model curve

Variables	Value	Variation
m_c	$(1.42 \pm 0.08) \text{ GeV}/c^2$	fitted
κ	0.38	± 0.10
α	1	± 1
ϵ_p^s	$0.083 \pm 0.013 \pm 0.010$	± 0.02
V_{cd}	0.221	fixed
V_{cs}	0.97437	fixed

The energy dependence can be compared with the prediction of charm production models. We used the structure function model in Ref. [45] (GRV94LO), with the parameters listed in Table 4. This parametrization includes slow rescaling [46], which is sensitive to the effective charm quark mass, m_c , and the parton distributions. In the determination of m_c , the most sensitive parameters are the relative fraction of the strange sea compared to the down-quark sea, κ , and the difference in the exponent of the x dependence of the strange and down sea, α . Fits to the observed energy dependence of the D^0 cross-section were performed using different sets of values of these parameters. The value of ϵ_p (the Peterson *et al.* [47] parameter) used corresponds with the measurement quoted for ϵ_p^s in Ref. [37] based on the same D^0 event sample, consistent with the convention used in the Lund model [35]. Values of the Cabibbo–Kobayashi–Maskawa matrix elements V_{cd} and V_{cs} were fixed at their known values [18]. The results of this fit are given in Table 4. We find a best fit value:

$$m_c = (1.42 \pm 0.08) \text{ GeV}/c^2, \quad (7)$$

where the error is statistical only. Variations of α and κ show derivatives of the best fit value which can be expressed as $\Delta(m_c) = (0.11 (\kappa - 0.38) - 0.06 (\alpha - 1)) \text{ GeV}/c^2$. Repeating the analysis with a variation of the value of ϵ_p within the errors quoted in Ref. [37] and with different sets of structure functions a systematic error of ± 0.04 is deduced. The experimental systematics is similar to this value.

In summary, using a high-statistics inclusive D^0 sample obtained by selecting decay topologies in an emulsion target, a measurement of branching ratios and of the production cross-section was performed. In particular, the ratio of D^0 branching fractions into four and two charged particles was determined to be $0.207 \pm 0.016 \pm 0.004$. Using the value quoted in the PDG [18] for the D^0 decay mode into four charged hadrons as normalization, the topological branchings into two and six charged particles were obtained as well as that into states containing only neutral daughters. The production cross-section relative to CC interactions was measured to be $0.0269 \pm 0.0018 \pm 0.0013$. From the energy dependence of this ratio a value of $(1.42 \pm 0.08) \text{ GeV}/c^2$ was extracted for the effective mass of the charm quark.

Acknowledgements

We gratefully acknowledge the help and support of the neutrino beam staff and of the numerous technical collaborators who contributed to the detector construction, operation, emulsion pouring, development, and scanning. The experiment was made possible by grants from the Institut Interuniversitaire des Sciences Nucléaires and the Interuniversitair Instituut voor Kernwetenschappen (Belgium), the Israel Science Foundation (grant 328/94) and the Technion Vice President Fund for the Promotion of Research (Israel), CERN (Geneva, Switzerland), the German Bundesministerium für Bildung und Forschung (Germany), the Institute of Theoretical and Experimental Physics (Moscow, Russia), the Istituto Nazionale di Fisica Nucleare (Italy), the Promotion and Mutual Aid Corporation for Private Schools of Japan and Japan Society for the Promotion of Science (Japan), the Korea Research Foundation Grant (KRF-2003-005-C00014) (Republic of Korea), the Foundation for Fundamental Research on Matter FOM and the National Scientific Research Organization NWO (The Netherlands), and the Scientific and Technical Research Council of Turkey (Turkey). We gratefully acknowledge their support.

References

- [1] H. Abramowicz *et al.*, CDHS Collaboration, *Z. Phys.* **C15** (1982) 19.
- [2] S.A. Rabinowitz *et al.*, CCFR Collaboration, *Phys. Rev. Lett.* **70** (1993) 134.
- [3] M. Jonker *et al.*, CHARM Collaboration, *Phys. Lett.* **B107** (1981) 241.
- [4] P. Vilain *et al.*, CHARM II Collaboration, *Eur. Phys. J.* **C11** (1999) 19.
- [5] M. Goncharov *et al.*, NuTeV Collaboration, *Phys. Rev.* **D64** (2001) 112006.
- [6] P. Astier *et al.*, NOMAD Collaboration, *Phys. Lett.* **B486**, (2000) 35.
- [7] P. Astier *et al.*, NOMAD Collaboration, *Phys. Lett.* **B526** (2002) 278.
- [8] A. Kayis-Topaksu *et al.*, CHORUS Collaboration, *Phys. Lett.* **B527** (2002) 173.
- [9] C. Angelini *et al.*, BEBC Collaboration, *Phys. Lett.* **B84** (1979) 150.
- [10] M. Calicchio *et al.*, BEBC-TST Collaboration, *Phys. Lett.* **B93** (1980) 521.
- [11] H. Grassler *et al.*, *Phys. Lett.* **99B** (1981) 159.
- [12] P.C. Bosetti *et al.*, *Phys. Lett.* **109B** (1981) 234.
- [13] D. Son *et al.*, *Phys. Rev. Lett.* **49** (1982) 1128.
- [14] Yu.A. Batusov *et al.*, *JETP Lett.* **46** (1987) 268; V.V. Ammosov *et al.*, *JETP Lett.* **58** (1993) 247.
- [15] A. Kayis-Topaksu *et al.*, CHORUS Collaboration, *Phys. Lett.* **B555** (2003) 156.
- [16] A. Kayis-Topaksu *et al.*, CHORUS Collaboration, *Phys. Lett.* **B575** (2003) 198.
- [17] J. M. Link *et al.*, FOCUS Collaboration, *Phys. Lett.* **B575** (2003) 190-197.
- [18] Particle Data Group, *Phys. Lett.* **B592** (2004).
- [19] C. G. Wohl, The sad state of charmed-particle branching fractions, PDG internal note, unpublished.
- [20] E. Eskut *et al.*, CHORUS Collaboration, *Nucl. Instrum. and Methods* **A401** (1997) 7.
- [21] S. Aoki *et al.*, *Nucl. Instrum. and Methods* **B51** (1990) 466.
- [22] T. Nakano. Ph.D. thesis, Nagoya University, Japan (1997).
- [23] M. Güler, Ph.D. thesis, METU, Ankara, Turkey (2000).
- [24] B. Van de Vyver, Ph.D. thesis, Vrije Universiteit Brussel, Brussels, Belgium, 2002. CERN-THESIS-2002-024.
- [25] T. Nakano, Proc. Int. Europhysics Conf. on High Energy Physics, Budapest, Hungary (2001).
- [26] K. Kodama *et al.*, *Nucl. Instrum. and Methods* **A493** (2002) 45.
- [27] N. Nonaka, Ph.D. thesis, Nagoya University, Japan (2002).
- [28] S. Sorrentino, Diploma Thesis, Naples University, Italy (1995).
- [29] GEANT 3.21, CERN program library long write up W5013.
- [30] G. Ambrosini *et al.*, SPY Collaboration, *Eur. Phys. J.* **C 10** (1999).
- [31] P. Astier *et al.*, NOMAD Collaboration, *Phys. Lett.* **B 570** 19-31 (2003).
- [32] I. Tsukerman, CHORUS Collaboration, MC generators in CHORUS, *Nucl. Phys. Proc. Suppl.* **112** (2002) 177.
- [33] P. Zucchelli, Ph.D. thesis, University of Ferrara, Italy (1996).
- [34] G. Ingelman, Preprint TSL/ISV 92-0065, Uppsala University, Sweden (1992).
- [35] T. Sjöstrand, *Comput. Phys. Commun.* **82** (1994) 74.
- [36] S. Ricciardi, Ph.D thesis, Università di Ferrara, Italy (1996).
- [37] G. Öngüt *et al.*, CHORUS Collaboration, *Phys. Lett.* **B604** (2004) 145.
- [38] P. Astier *et al.*, NOMAD Collaboration, *Nucl. Phys.* **B621** (2002) 3.
- [39] M. Sorrentino, CHORUS internal note 2000027 (2004),
http://choruswww.cern.ch/Publications/Notes/charm_background.pdf
- [40] G.J. Feldman and R.D. Cousins, *Phys. Rev.* **D57** (1998) 3873.
- [41] S. Barlag *et al.*, ACCMOR Collaboration, *Z. Phys.* **C55** (1992) 383; **C48** (1990) 29.
- [42] J.M. Link *et al.*, FOCUS Collaboration, *Phys. Lett.* **B586** (2004) 21.
- [43] A. Artamonov and P. Gorbunov, CHORUS Internal Note 97029, 23 February 1998, updated 12 March 1999. http://choruswww.cern.ch/Publications/Notes/spec1mu_new.pdf
- [44] N. Ushida, *et al.*, E531 Collaboration, *Phys. Lett.* **B 206** (1988) 375.
- [45] M. Glück, E. Reya and A. Vogt, *Z. Phys.* **C** (1995) 433.
- [46] M.A.G. Aivazis *et al.*, *Phys. Rev.* **D50** (1994) 3085; **D50** (1994) 3102.
- [47] C. Peterson *et al.*, *Phys. Rev.* **D27** (1983) 105.